ELSEVIER

Journal of Organometallic Chemistry 645 (2002) 235–245

Journal of Organometallic Chemistry

www.elsevier.com/locate/jorganchem

Syntheses and structures of dimethylamino-bridged bis(silylene)ruthenium and -osmium complexes

Tong N. Choo, Wai-Him Kwok, Clifton E.F. Rickard, Warren R. Roper *, L. James Wright *

Department of Chemistry, The University of Auckland, Private Bag 92019 Auckland, New Zealand

Received 24 August 2001; accepted 29 September 2001

Abstract

Treatment of $Os(SiMe_2Cl)Cl(CO)(PPh_3)_2$ with an excess of the amino-substituted silane, $HSiMe_2NMe_2$, produces a mixture of two products, the relative proportions of which depend upon the reaction conditions. These are, $Os(SiMe_2NMe_2SiMe_2)Cl(CO)(PPh_3)_2$ (**1**) and $Os(SiMe_2NMe_2SiMe_2)H(CO)(PPh_3)_2$ (**2**). Similar treatment of $Ru(SiMe_2Cl)Cl(CO)(PPh_3)_2$ with $HSiMe_2NMe_2$ produces the ruthenium analogues of **1** and **2**, $Ru(SiMe_2NMe_2SiMe_2)Cl(CO)(PPh_3)_2$ (**3**), and $Ru(SiMe_2NMe_2SiMe_2)H(CO)(PPh_3)_2$ (**4**), together with a third compound, the novel dimethylsilylene-bridged diruthenium complex, $[Ru(SiMe_2NMe_2SiMe_2)(CO)(\mu\text{-}\{SiMe_2\})_2(\mu\text{-}Cl)RuH_2(CO)(PPh_3)]$ (**5**). A ligand exchange reaction occurs when **3** is treated with 1,2-bis(diphenylphosphino)ethane (dppe) yielding $Ru(SiMe_2NMe_2SiMe_2)Cl(CO)(dppe)$ (**6**), in which the bis(silylene) ligand is retained. Crystal structures of **1**, **2**, **4**, and **6** reveal that the RuSiNSi and OsSiNSi rings of the bis(silylene) ligand system are folded at the Si atoms and the Ru–Si and Os–Si distances are short, while Si–N distances are long. These structural data suggest some multiple bond character in the metal–silicon bonds and this is further supported by the down-field chemical shifts observed in the ^{29}Si-NMR spectra of these compounds. A crystal structure has also been determined for the diruthenium complex **5** and this reveals a Ru–Ru distance of 2.7557(2) Å, and two unsymmetrically bridging dimethylsilylene ligands each with a close approach to one of the ruthenium hydride ligands (Si–H, 1.56(2) and 1.67(2) Å).

Keywords: Silylene complexes; Osmium; Ruthenium; X-ray crystal structures; Dinuclear complexes

1. Introduction

The study of transition metal silylene complexes has become an active area of research in the past two decades. These species have been proposed as the reactive intermediates in a variety of chemical reactions [1] and transition metal mediated processes including Rochow's direct process [2], catalytic redistribution of silanes [3], and dehydrogenative silane coupling [4]. Both donor-stabilised and donor-free transition metal silylene complexes have been isolated and fully characterised. Examples from Tilley and co-workers are provided by the acetonitrile-stabilised ruthenium silylene species $[Cp^*(Me_3P)_2Ru{=}SiPh_2{\cdot}NCCH_3]^+$ [5], and the donor-free silylene complexes of the type $[Cp^*(Me_3P)_2Ru{=}SiR_2]BPh_4$ (R = SR, Me or Ph) [6]. Metal complexes of the stable bis(amino)silylenes have also been prepared and this subject has been reviewed recently [6c,d]. A special class of donor-stabilised silylene complexes, which has been extensively studied by Ogino and co-workers, involves a donor-bridged bis(silylene) arrangement as illustrated in Fig. 1. The metals examined include Cr, Mo, W, Mn, Fe, Ru, and Ir while the bridging donor group may be OMe, O^{t}Bu, and NEt_2. These have all been prepared by the rear-

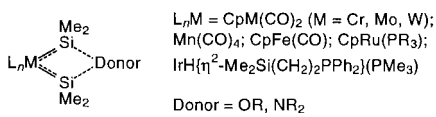

Fig. 1. Donor-bridged bis(silylene)metal complexes.

* Corresponding authors. Tel.: +64-9-373-7999x8320; fax: +64-9-373-7422.

E-mail address: w.roper@auckland.ac.nz (W.R. Roper).

0022-328X/02/$ - see front matter © 2002 Elsevier Science B.V. All rights reserved.
PII: S0022-328X(01)01331-6

Table 1
Crystal data and structure refinement parameters for **1**, **2**, **4**–**6**

	1	**2**	**4**	**5**	**6**
Empirical formula	$C_{43}H_{48}ClNOOsP_2Si_2 \cdot C_6H_6$	$C_{43}H_{49}NOP_2OsSi_2 \cdot (C_6H_6)_2$	$C_{43}H_{49}NOP_2RuSi_2 \cdot (C_6H_6)_2$	$C_{30}H_{47}ClNO_2PRu_2Si_4$	$C_{33}H_{42}ClNOP_2RuSi_2$
Formula weight	1016.70	1060.37	971.24	834.61	723.32
Temperature (K)	150	150	150	150	150
Wavelength (Å)	0.71073	0.71073	0.71073	0.71073	0.71073
Crystal system	Monoclinic	Triclinic	Triclinic	Monoclinic	Monoclinic
Space group	*Cc*	$P\bar{1}$	$P\bar{1}$	$P2_1/n$	$P2_1/c$
Unit cell dimensions					
a (Å)	20.6926(4)	12.9960(1)	13.0158(1)	9.9566(1)	8.8727(1)
b (Å)	11.1430(2)	13.5828(1)	13.5952(2)	28.0421(3)	17.9427(2)
c (Å)	22.9687(5)	14.3220(1)	14.3118(1)	13.6412(1)	21.5360(3)
α (°)	90.0	92.856(1)	93.013(1)	90.0	90.0
β (°)	107.362(1)	90.839(1)	90.763(1)	97.190(1)	99.115(1)
γ (°)	90.0	97.741(1)	97.680(1)	90.0	90.0
V (Å^3)	5054.77(17)	2501.42(3)	2505.82(5)	3771.22(6)	3384.24(7)
Z	4	2	2	4	4
D_{calc} (g cm^{-3})	1.336	1.408	1.287	1.470	1.419
$F(000)$	2056	1080	1016	1704	1497
μ (mm^{-1})	2.720	2.699	0.463	1.068	0.734
Crystal size (mm)	$0.55 \times 0.29 \times 0.22$	$0.40 \times 0.19 \times 0.15$	$0.40 \times 0.22 \times 0.09$	$0.45 \times 0.30 \times 0.22$	$0.54 \times 0.50 \times 0.38$
2θ (min/max) (°)	1.8/27.5	1.4/27.5	1.4/27.4	1.4/27.5	1.5/27.5
Index range	$-16 \le h \le 26$, $0 \le k \le 14$, $-29 \le l \le 25$	$-16 \le h \le 16$, $-17 \le k \le 17$, $0 \le l \le 18$	$-16 \le h \le 16$, $-17 \le k \le 17$, $0 \le l \le 18$	$-12 \le h \le 12$, $0 \le k \le 35$, $0 \le l \le 17$	$-11 \le h \le 11$, $0 \le k \le 22$, $0 \le l \le 27$
Reflections collected	15 477	24 292	24 723	22 810	18 850
Independent reflections	8217 [$R_{int} = 0.0257$]	10 771	10 814 [$R_{int} = 0.0248$]	8328 [$R_{int} = 0.156$]	7383
A (min/max)	0.316, 0.586	0.411, 0.687	0.836, 0.959	0.645, 0.799	0.693, 0.768
Function minimised	$\Sigma w(F_o^2 - F_c^2)^2$	$\Sigma w(F_o^2 - F_c^2)^2$	$\Sigma w(F_o^2 - F_c^2)^2$	$\Sigma w(F_o^2 - F_c^2)^2$	$\Sigma w(F_o^2 - F_c^2)^2$
Observed data/parameters	7667/520	9852/568	9258/568	7534/386	6481/376
Goodness-of-fit on F^2	1.126	1.014	1.042	1.045	1.115
R (observed data)	$R_1 = 0.0351$, $wR_2 = 0.1063$	$R_1 = 0.0208$, $wR_2 = 0.0491$	$R_1 = 0.0317$, $wR_2 = 0.0657$	$R_1 = 0.0238$, $wR_2 = 0.0546$	$R_1 = 0.0310$, $wR_2 = 0.0751$
R (all data)	$R_1 = 0.0385$, $wR_2 = 0.1102$	$R_1 = 0.0259$, $wR_2 = 0.0516$	$R_1 = 0.0433$, $wR_2 = 0.0717$	$R_1 = 0.0282$, $wR_2 = 0.0565$	$R_1 = 0.0379$, $wR_2 = 0.0806$
Least-squares weights a and b	0.069, 10.711	0.025, 1.147	0.018, 1.979	0.024, 3.446	0.033, 3.472
Largest difference between peak and hole (e Å^{-3})	+1.53 and −0.98	+1.04 and −0.48	+0.34 and −0.40	+1.60 and −0.70	+0.39 and −0.79

$R = \Sigma||F_o| - |F_c||/\Sigma|F_o|$, $wR_2 = \{\Sigma[w(F_o^2 - F_c^2)^2]/\Sigma[w(F_o^2)^2]\}^{1/2}$ weight $= 1.0/[\sigma^2(F_o^2) + aP^2 + bP]$ where $P = (F_o^2 + 2F_c^2)/3$.

rangement of an intermediate disilanyl complex of the type, L_nM–$SiMe_2SiMe_2$Donor [7a–e], e.g. through photolysis of (alkoxydisilanyl)carbonyliron and -manganese complexes or by the thermal reaction of $CpRu(PPh_3)_2Me$ with $HMe_2SiSiMe_2OMe$ [7f].

Herein, we report: (i) the syntheses of dimethylamino-bridged bis(silylene)ruthenium and -osmium complexes which utilise excess $HSiMe_2NMe_2$ as the precursor to the bis(silylene) ligand system, thereby avoiding prior synthesis of disilanyl complexes; (ii) stable compounds which incorporate a hydride ligand adjacent to the bis(silylene) ligand system (from the same reaction mixtures); (iii) an unusual diruthenium complex incorporating the same bis(silylene) ligand in addition to two bridging dimethylsilylene ligands; (iv) simple phosphine ligand exchange which leaves the bis(silylene) ligand unaltered, and (v) spectral data and crystal structure determinations (Table 1) of all of the above products.

2. Results and discussion

2.1. Syntheses and structures of dimethylamino-bridged bis(silylene)osmium complexes

As depicted in Scheme 1, reaction between $Os(SiMe_2Cl)Cl(CO)(PPh_3)_2$ and excess $HSiMe_2NMe_2$, leads to a mixture of the two dimethylamino-bridged bis(silylene) complexes, $\overline{Os(SiMe_2NMe_2SiMe_2)}Cl(CO)(PPh_3)_2$ (**1**), and $\overline{Os(SiMe_2NMe_2SiMe_2)}H(CO)(PPh_3)_2$ (**2**). The yield of **1** is maximised when the reaction is carried out in benzene solution at a temperature of 75 °C for 21 h. The yield of **2** is maximised when the

reaction is carried out in benzene solution at a temperature of 90 °C for 24 h. Both sets of reaction conditions produce **1** and **2** but these two compounds are easily separated by fractional crystallisation.

Complexes **1** and **2** have been fully characterised by IR and NMR spectroscopic methods, by elemental analysis, and by X-ray crystallography. Complex **1** has a ν(CO) at 1890 cm^{-1} in the IR spectrum. Both ^{1}H- and ^{13}C-NMR spectra reveal two environments for the methyl groups resident on silicon and for the methyl groups resident on nitrogen. The ^{29}Si-NMR shows one signal only for the two silicon atoms (at 37.85 ppm). The multiplicity of this signal is a doublet of doublets through coupling to phosphorus as expected for a geometry with the two triphenylphosphine ligands mutually *cis* and lying in the same plane as the osmium and the two silicon atoms of the bis(silylene) ligand. The molecular geometry of **1** as determined by X-ray crystallography is shown in Fig. 2 and selected bond distances and angles are presented in Table 2. The structure has two mutually *cis* triphenylphosphine ligands, the chloride and carbonyl ligands are mutually *trans* and the remaining two coordination sites at the osmium are occupied by the dimethylamino-bridged bis(silylene) ligand. The complexes, $L_nM(SiMe_2NEt_2SiMe_2)$, with a closely related bis(silylene) ligand, have been obtained previously from photolytically induced

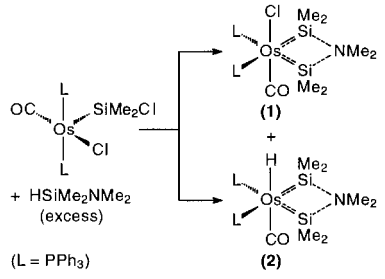

Scheme 1. Syntheses of dimethylamino-bridged bis(silylene)-osmium(II) complexes.

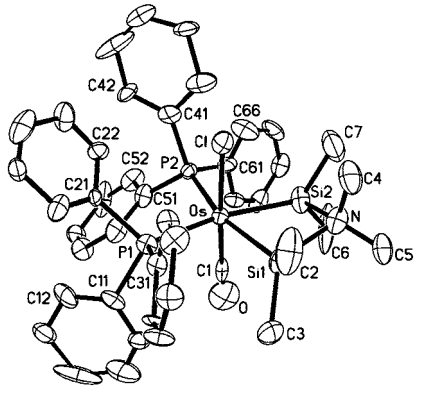

Fig. 2. Molecular geometry of $Os(SiMe_2NMe_2SiMe_2)Cl(CO)(PPh_3)_2$ (**1**).

Table 2
Selected bond lengths (Å) and bond angles (°) for **1**

Bond lengths	
Os–C(1)	1.99(2)
Os–Si(2)	2.393(4)
Os–Si(1)	2.432(4)
Os–P(2)	2.451(3)
Os–P(1)	2.456(4)
Os–Cl	2.511(4)
Si(1)–C(2)	1.86(2)
Si(1)–C(3)	1.940(11)
Si(1)–N	2.007(9)
Si(2)–C(6)	1.841(17)
Si(2)–N	1.859(9)
Si(2)–C(7)	1.864(13)
N–C(5)	1.443(14)
N–C(4)	1.500(15)
Bond angles	
C(1)–Os–Si(2)	87.4(3)
C(1)–Os–Si(1)	88.9(3)
Si(2)–Os–Si(1)	68.83(6)
C(1)–Os–P(2)	86.0(3)
Si(2)–Os–P(2)	92.91(13)
Si(1)–Os–P(2)	161.27(12)
C(1)–Os–P(1)	96.3(3)
Si(2)–Os–P(1)	161.99(13)
Si(1)–Os–P(1)	93.56(13)
P(2)–Os–P(1)	104.91(5)
C(1)–Os–Cl	177.1(3)
Si(2)–Os–Cl	89.81(15)
Si(1)–Os–Cl	89.39(15)
P(2)–Os–Cl	94.82(14)
P(1)–Os–Cl	86.15(14)
C(2)–Si(1)–C(3)	91.5(9)
C(2)–Si(1)–N	95.6(7)
C(3)–Si(1)–N	131.0(5)
C(2)–Si(1)–Os	125.0(7)
C(3)–Si(1)–Os	119.3(4)
N–Si(1)–Os	95.5(3)
C(6)–Si(2)–N	106.2(7)
C(6)–Si(2)–C(7)	116.3(9)
N–Si(2)–C(7)	72.3(5)
C(6)–Si(2)–Os	123.2(7)
N–Si(2)–Os	100.9(3)
C(7)–Si(2)–Os	119.2(4)
C(5)–N–C(4)	101.2(11)
C(5)–N–Si(2)	129.5(12)
C(4)–N–Si(2)	112.1(7)
C(5)–N–Si(1)	111.9(11)
C(4)–N–Si(1)	112.3(6)
Si(2)–N–Si(1)	89.7(3)

rearrangement of $L_nMSiMe_2SiMe_2NEt_2$ [7g,h]. The four-membered OsSiNSi ring in **1** is non-planar with the dihedral angle between the Si(1)–Os–Si(2) plane and the Si(1)–N–Si(2) plane being 22.4(3)°. Closely similar values are found for the corresponding dihedral angles in complexes **2** (24.19(7)°), **4** (23.79(6)°), **5** (24.2(1)°), and **6** (23.2(1)°) described below. The previously reported Group 6 complexes with diethylamino-bridged bis(silylene) ligands also have non-planar four-membered rings with similar dihedral angles [7g,h]. The

Os–Si distances in **1** are short (Os–Si(1), 2.393(4); Os–Si(2), 2.432(4) Å) when compared with other Os–Si distances where the silicon is *trans* to triphenylphosphine in an octahedral osmium(II) complex, e.g. in $Os(SiEt_3)H(CO)_2(PPh_3)_2$ the Os–Si distance is 2.493(2) Å [8]. The Si–N distances are very long (Si(1)–N, 2.007(9); Si(2)–N, 1.859(9) Å) compared with normal Si–N single bonds (1.70–1.76 Å). Again these features are observed in all the structures reported here and suggest contributions to the bonding from the valence bond structures depicted in Fig. 3.

$\overline{Os(SiMe_2NMe_2SiMe_2)}H(CO)(PPh_3)_2$ (**2**) has ν(CO) at 1859 cm^{-1} and ν(OsH) at 1964 cm^{-1} in the IR spectrum. In the ^{1}H-NMR spectrum the hydride signal appears as a triplet at -7.69 ppm, but in other respects the ^{1}H-, ^{13}C-, and ^{29}Si-NMR spectra of **2** are very similar to those of complex **1**. These observations are compatible with the hydride replacing chloride without other geometrical change about the metal. This is confirmed by a crystal structure determination. The molecular geometry of **2** is shown in Fig. 4 and selected bond distances and angles are presented in Table 3. The Os–H distance is 1.61(2) Å and the structural parameters associated with the bis(silylene) ligand are closely similar to those observed for complex **1**.

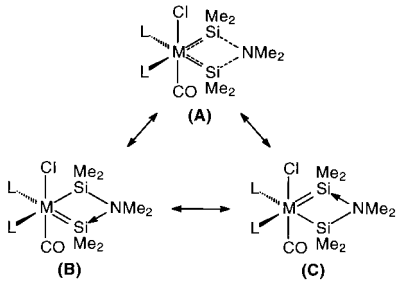

Fig. 3. Valence bond structures for dimethylamino-bridged bis(silylene)metal complexes.

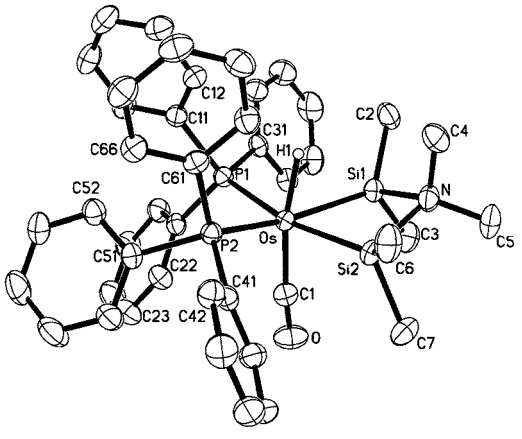

Fig. 4. Molecular geometry of $\overline{Os(SiMe_2NMe_2SiMe_2)}H(CO)(PPh_3)_2$ (**2**).

Table 3
Selected bond lengths (Å) and bond angles (°) for **2**

Bond lengths	
Os–C(1)	1.892(3)
Os–P(1)	2.3762(6)
Os–P(2)	2.3810(6)
Os–Si(1)	2.3929(7)
Os–Si(2)	2.4024(6)
Os–H	1.61(2)
Si(1)–C(2)	1.886(3)
Si(1)–C(3)	1.892(3)
Si(1)–N	1.944(2)
Si(2)–C(7)	1.896(3)
Si(2)–C(6)	1.900(3)
Si(2)–N	1.923(2)
N–C(5)	1.485(3)
N–C(4)	1.495(3)
Bond angles	
C(1)–Os–P(1)	95.26(7)
C(1)–Os–P(2)	103.68(8)
P(1)–Os–P(2)	97.63(2)
C(1)–Os–Si(1)	93.55(8)
P(1)–Os–Si(1)	97.09(2)
P(2)–Os–Si(1)	156.13(2)
C(1)–Os–Si(2)	89.41(7)
P(1)–Os–Si(2)	166.11(2)
P(2)–Os–Si(2)	93.94(2)
Si(1)–Os–Si(2)	69.52(2)
C(2)–Si(1)–C(3)	103.45(13)
C(2)–Si(1)–N	103.09(11)
C(3)–Si(1)–N	102.27(11)
C(2)–Si(1)–Os	124.89(9)
C(3)–Si(1)–Os	121.47(10)
N–Si(1)–Os	97.15(7)
C(7)–Si(2)–C(6)	102.51(14)
C(7)–Si(2)–N	102.59(12)
C(6)–Si(2)–N	103.98(12)
C(7)–Si(2)–Os	118.20(10)
C(6)–Si(2)–Os	128.09(9)
N–Si(2)–Os	97.41(6)
C(5)–N–C(4)	107.6(2)
C(5)–N–Si(2)	118.70(18)
C(4)–N–Si(2)	110.69(17)
C(5)–N–Si(1)	118.29(17)
C(4)–N–Si(1)	110.74(16)
Si(2)–N–Si(1)	89.97(9)

2.2. Syntheses and structures of dimethylamino-bridged bis(silylene)ruthenium complexes

As depicted in Scheme 2, reaction between $Ru(SiMe_2Cl)Cl(CO)(PPh_3)_2$ and excess $HSiMe_2NMe_2$, leads to the three dimethylamino-bridged bis(silylene) complexes, $\overline{Ru(SiMe_2NMe_2SiMe_2)}Cl(CO)(PPh_3)_2$ (**3**), $\overline{Ru(SiMe_2NMe_2SiMe_2)}H(CO)(PPh_3)_2$ (**4**), and $[\overline{Ru(SiMe_2NMe_2SiMe_2)}(CO)(\mu\text{-}\{SiMe_2\})_2(\mu\text{-}Cl)RuH_2(CO)(PPh_3)]$ (**5**). The yield of **3** is maximised when the reaction is carried out in benzene solution at a temperature of 70 °C for 18 h. The yield of **4** is maximised when the reaction is carried out in benzene solution at

a temperature of 80 °C for 24 h. Both sets of reaction conditions produce both **3** and **4**, but these two compounds are easily separated by fractional crystallisation. The more soluble, orange-coloured **5**, can be separated from the reaction mixtures after removal of the less soluble **3** and **4**.

Complexes **3**–**5** have been fully characterised by IR and NMR spectroscopic methods, by elemental analysis, and for **4** and **5** also by X-ray crystallography (see below). All the spectroscopic data are consistent with compounds **3**–**5** having the structures shown in Scheme 2. Complex **3** has a ν(CO) at 1895 cm^{-1} in the IR spectrum. As discussed above for complexes **1** and **2**, both ^{1}H- and ^{13}C-NMR spectra reveal two environments for the methyl groups resident on silicon and for the methyl groups resident on nitrogen. The ^{29}Si-NMR spectrum shows a doublet of doublets signal for the two silicon atoms at 59.83 ppm. The crystal structure of **3** was plagued by poor data and disorder problems and is not reported here but the compound is clearly isostructural with the osmium analogue, **1**.

$\overline{Ru(SiMe_2NMe_2Si}Me_2)H(CO)(PPh_3)_2$ (**4**) has ν(CO) at 1918 cm^{-1} and ν(RuH) at 1828 cm^{-1} in the IR spectrum. In the ^{1}H-NMR spectrum the hydride signal appears as a triplet at -6.78 ppm but in other respects the ^{1}H-, ^{13}C-, and ^{29}Si-NMR spectra of **4** are very similar to those observed for complexes **1**–**3**. These observations are compatible with the hydride replacing chloride without other geometrical change about the metal. This is confirmed by a crystal structure determination which shows that **4** is isostructural with **2**. A separate molecular structure diagram is therefore not shown for **4** but selected bond distances and angles are presented in Table 4. The Ru–H distance is 1.62(2) Å and the structural parameters associated with the bis(silylene) ligand are closely similar to those observed in all the other complexes.

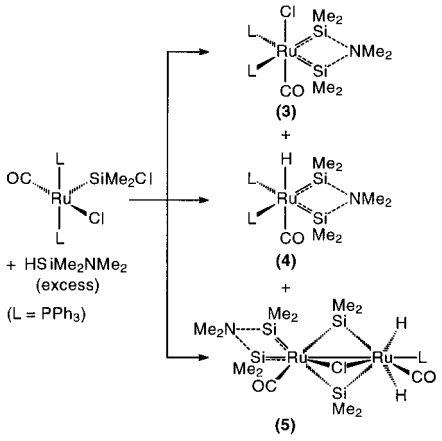

Scheme 2. Syntheses of dimethylamino-bridged bis(silylene)-ruthenium(II) complexes.

Table 4
Selected bond lengths (Å) and bond angles (°) for **4**

Bond lengths	
Ru–C(1)	1.892(2)
Ru–Si(1)	2.3702(6)
Ru–Si(2)	2.3821(6)
Ru–P(1)	2.3860(5)
Ru–P(2)	2.3983(5)
Ru–H	1.62(2)
Si(1)–C(2)	1.892(2)
Si(1)–C(3)	1.906(2)
Si(1)–N	1.9420(19)
Si(2)–C(6)	1.901(2)
Si(2)–C(7)	1.902(2)
Si(2)–N	1.9264(18)
N–C(5)	1.494(3)
N–C(4)	1.497(3)
Bond angles	
C(1)–Ru–Si(1)	93.51(7)
C(1)–Ru–Si(2)	89.50(7)
Si(1)–Ru–Si(2)	69.72(2)
C(1)–Ru–P(1)	95.42(7)
Si(1)–Ru–P(1)	97.025(19)
Si(2)–Ru–P(1)	166.173(19)
C(1)–Ru–P(2)	104.71(6)
Si(1)–Ru–P(2)	155.53(2)
Si(2)–Ru–P(2)	93.861(19)
P(1)–Ru–P(2)	97.353(18)
C(2)–Si(1)–C(3)	102.93(11)
C(2)–Si(1)–N	103.31(9)
C(3)–Si(1)–N	102.37(9)
C(2)–Si(1)–Ru	125.04(8)
C(3)–Si(1)–Ru	121.30(8)
N–Si(1)–Ru	97.63(6)
C(6)–Si(2)–C(7)	102.18(12)
C(6)–Si(2)–N	103.71(10)
C(7)–Si(2)–N	102.68(10)
C(6)–Si(2)–Ru	128.10(8)
C(7)–Si(2)–Ru	118.45(8)
N–Si(2)–Ru	97.68(6)
C(5)–N–C(4)	107.50(17)
C(5)–N–Si(2)	118.61(15)
C(4)–N–Si(2)	110.71(14)
C(5)–N–Si(1)	118.53(15)
C(4)–N–Si(1)	111.40(14)
Si(2)–N–Si(1)	89.21(7)

The formation of the dimethylamino-bridged bis(silylene) ligand in all of complexes **1**–**4**, can be understood by the proposed sequence of reactions shown in Scheme 3. The first step involves exchange of the dimethylchlorosilyl ligand with the dimethylaminodimethylsilyl ligand (compound **D** in Scheme 3). A precedent for this kind of exchange process is provided by the preparation of $Ru(SiPh_3)Cl(CO)(PPh_3)_2$ from treatment of $Ru(SiMe_3)Cl(CO)(PPh_3)_2$ with $HSiPh_3$ [9]. Addition of $HSiMe_2NMe_2$ to **D** could give intermediate **E** which upon rearrangement could produce the dimethylamine-stabilised dimethylsilylene complex **F**. Intramolecular replacement of the dimethylamine by the dimethylamino group on the adjacent

dimethylaminodimethylsilyl ligand would give the observed products **1** and **3** containing the dimethylamino-bridged bis(silylene) ligand.

Complexes **2** and **4** in which the chloride ligand is replaced by hydride could arise from reaction of **1** and **3** with excess $HSiMe_2NMe_2$ through an oxidative addition/reductive elimination sequence. It is interesting to note the high stability of **2** and **4** in view of the fact that the hydride ligand is located *cis* to the bis(silylene) ligand where there is the opportunity for hydride migration to an adjacent silicon donor atom, resulting in either Me_2HSi-ligand formation or reductive elimination of a silane. A further indication of the robustness of the bis(silylene) ligand system is that this remains intact during the replacement of the two triphenylphosphine ligands by 1,2-bis(diphenylphosphino)ethane (dppe). $\overline{Ru(SiMe_2NMe_2SiMe_2)}Cl(CO)(PPh_3)_2$ (**3**), when treated with dppe, produces $\overline{Ru(SiMe_2NMe_2SiMe_2)}$-Cl(CO)(dppe) (**6**) (see Scheme 4). The spectroscopic data for **6** are, as expected, closely similar to those of complexes **1**–**4**. The molecular structure of **6** is depicted

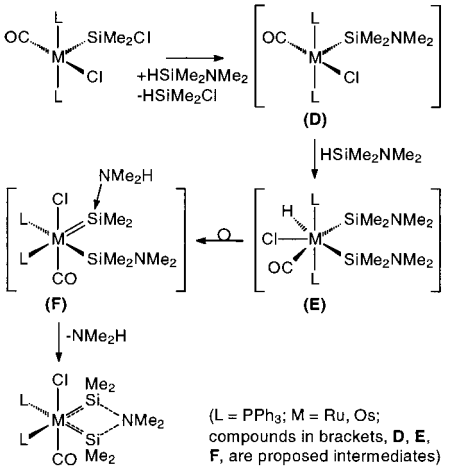

Scheme 3. Suggested mechanism for formation of dimethylamino-bridged bis(silylene)ruthenium(II) and -osmium(II) complexes.

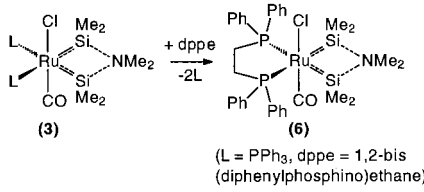

Scheme 4. Phosphine ligand exchange reaction.

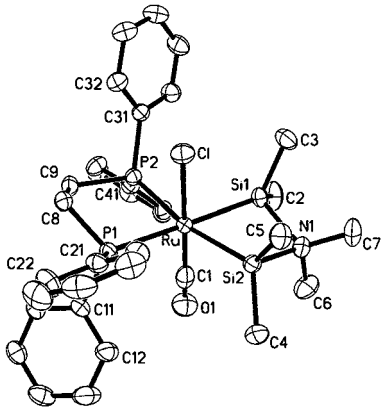

Fig. 5. Molecular geometry of $\overline{Ru(SiMe_2NMe_2SiMe_2)}Cl(CO)(dppe)$ (**6**).

Table 5
Selected bond lengths (Å) and bond angles (°) for **6**

Bond lengths	
Ru–C(1)	1.884(3)
Ru–Si(1)	2.3732(6)
Ru–P(2)	2.3781(6)
Ru–Si(2)	2.3883(6)
Ru–P(1)	2.3886(6)
Ru–Cl	2.4870(6)
Si(1)–C(2)	1.870(3)
Si(1)–C(3)	1.875(3)
Si(1)–N(1)	1.908(2)
Si(2)–C(4)	1.877(3)
Si(2)–C(5)	1.881(3)
Si(2)–N(1)	1.927(2)
N(1)–C(7)	1.493(3)
N(1)–C(6)	1.499(3)
Bond angles	
C(1)–Ru–Si(1)	91.47(8)
C(1)–Ru–P(2)	95.26(8)
Si(1)–Ru–P(2)	99.75(2)
C(1)–Ru–Si(2)	88.56(8)
Si(1)–Ru–Si(2)	68.98(2)
P(2)–Ru–Si(2)	168.24(2)
C(1)–Ru–P(1)	93.35(8)
Si(1)–Ru–P(1)	173.75(2)
P(2)–Ru–P(1)	83.78(2)
Si(2)–Ru–P(1)	107.14(2)
C(1)–Ru–Cl	177.51(8)
Si(1)–Ru–Cl	90.27(2)
P(2)–Ru–Cl	86.20(2)
Si(2)–Ru–Cl	90.39(2)
P(1)–Ru–Cl	84.79(2)
C(2)–Si(1)–C(3)	104.13(14)
C(2)–Si(1)–N(1)	104.51(12)
C(3)–Si(1)–N(1)	103.61(11)
C(2)–Si(1)–Ru	125.26(9)
C(3)–Si(1)–Ru	117.60(9)
N(1)–Si(1)–Ru	98.62(7)
C(4)–Si(2)–C(5)	104.00(13)
C(4)–Si(2)–N(1)	105.77(12)
C(5)–Si(2)–N(1)	102.40(11)
C(4)–Si(2)–Ru	122.90(10)
C(5)–Si(2)–Ru	120.88(9)
N(1)–Si(2)–Ru	97.55(6)
C(7)–N(1)–C(6)	106.6(2)
C(7)–N(1)–Si(1)	117.15(17)
C(6)–N(1)–Si(1)	111.70(17)
C(7)–N(1)–Si(2)	120.30(17)
C(6)–N(1)–Si(2)	111.06(17)
Si(1)–N(1)–Si(2)	89.34(9)

in Fig. 5 and selected bond distances and angles are presented in Table 5. All features are as expected and require no further comment.

2.3. Spectroscopic and structural characterisation of the dinuclear complex, [Ru(SiMe$_2$NMe$_2$SiMe$_2$)(CO)(μ-{SiMe$_2$})$_2$(μ-Cl)RuH$_2$(CO)(PPh$_3$)] (5)

The orange crystalline compound, [Ru(SiMe$_2$NMe$_2$SiMe$_2$)(CO)(μ-{SiMe$_2$})$_2$(μ-Cl)RuH$_2$(CO)(PPh$_3$)] (**5**), has a novel dinuclear structure the nature of which was fully revealed by a single crystal structure determination and the details of this will be discussed below. The three bridging ligands are chloride, and two dimethylsilylene units. In addition to the bridging ligands one ruthenium has a dimethylamino-bridged bis(silylene) ligand (as is present in complexes **1**–**4**, and **6**), together with one terminal CO ligand. The non-bridging ligands on the second ruthenium are one triphenylphosphine, one CO, and two hydride ligands (see Scheme 2). Complex **5** has two very strong bands in the IR spectrum at 1962 and 1896 cm^{-1} which must be associated with ν(CO). The ^{1}H-NMR spectrum shows two signals for both the N–CH$_3$ and Si–CH$_3$ groups of the bis(silylene) ligand and likewise two methyl signals for the bridging dimethylsilylene ligands. This is as expected from examination of the structure. There is also a high-field proton resonance at δ, −6.37 ppm, which is a doublet ($^2J_{HP}$ = 7.2 Hz) and which integrates for two protons. This indicates that both hydrides are equivalent and resident on the ruthenium atom which also carries the triphenylphosphine ligand. The chemical shift for the hydride ligands in complex **5** is very similar to that observed for complex **4** (δ −6.78 ppm) but the H–P coupling constant in **5** is much smaller than that observed in **4** ($^2J_{HP}$ = 16.2 Hz). This is compatible with the structural results to be discussed below. The ^{13}C-NMR spectrum confirms that there are two methyl environments for both the N–CH$_3$ and the Si–CH$_3$ groups of the bis(silylene) ligand, but all four methyl groups of the bridging dimethylsilylene ligands have different chemical shifts (δ 4.94, 4.97, 10.05, 10.10 ppm). In the ^{29}Si-NMR spectrum the singlet resonance at δ 71.05 ppm is assigned to the bis(silylene) ligand and the doublet at δ 148.60 ppm ($^2J_{SiP}$ = 35.8 Hz) to the bridging dimethylsilylene ligands.

A detailed examination of the structure of **5** as revealed by X-ray crystallography gives valuable insight into the bonding interactions in this dinuclear molecule. The molecular geometry is shown in Fig. 6 and selected bond distances and angles are presented in Table 6. The structural parameters of the dimethylamino-bridged bis(silylene) ligand on Ru(2) are closely similar to those observed for complexes **1**, **2**, **4**, and **6** and require no further comment. The Ru(1)–Ru(2) distance is 2.7557(2) Å and this is at the lower end of measured Ru–Ru distances which have a mean of 2.846 Å with a standard deviation of 0.112 Å [10]. If this Ru–Ru interaction is regarded as a 2c-2e bond the formal electron count at each Ru atom becomes 18. In keeping with this, complex **5** was recovered unchanged after exposure to CO, i.e. each Ru centre is coordinatively saturated. Of the three bridging ligands, chloride is more or less symmetrically bridging (Ru(1)–Cl, 2.5307(5); Ru(2)–Cl, 2.5232(5) Å) but the two dimethylsilylene ligands bridge in a distinctly unsymmetrical fashion (Ru(1)–Si(1), 2.5678(6); Ru(2)–Si(1), 2.3781(6); Ru(1)–Si(2), 2.5624(6); Ru(2)–Si(2), 2.3822(6) Å). Clearly, the direct Ru(2)–Si interactions are stronger than the corresponding Ru(1)–Si interactions. The reasons for this become clear when the positions of the hydrogen atoms are considered. Both hydrogen atoms were observed and refined in the crystal structure and were found on Ru(1), arranged mutually *trans* (H(1)–Ru(1)–H(2), 179.3(9)°) with Ru(1)–H(1), 1.66(2) and Ru(1)–H(2), 1.69(2) Å. These distances are slightly longer than the Ru–H distance of 1.62(2) Å found in complex **4** and longer than the mean of measured non-bridging Ru–H bonds (mean Ru–H, 1.584 Å; SD sample, 0.126 Å) [10]. Furthermore, each hydride makes a close approach to one of the bridging dimethylsilylene Si atoms. These distances are:

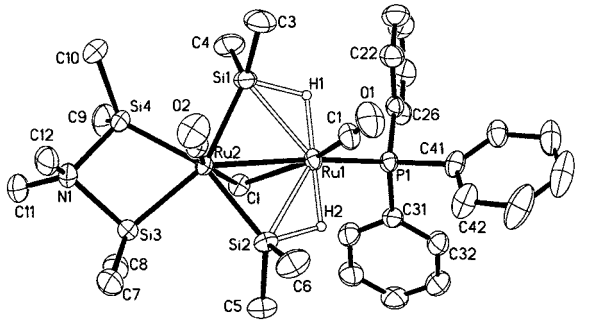

Fig. 6. Molecular geometry of [Ru(SiMe$_2$NMe$_2$SiMe$_2$)(CO)(μ-{SiMe$_2$})$_2$(μ-Cl)RuH$_2$(CO)(PPh$_3$)] (**5**).

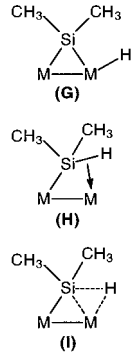

Fig. 7. A portion of the structure of **5** showing alternative valence bond formulations for the adjacent bridging dimethylsilylene ligand and the terminal Ru–H.

Table 6
Selected bond lengths (Å) and bond angles (°) for **5**

Bond lengths	
Ru(1)–C(1)	1.825(2)
Ru(1)–P(1)	2.3419(5)
Ru(1)–Cl	2.5307(5)
Ru(1)–Si(2)	2.5624(6)
Ru(1)–Si(1)	2.5678(6)
Ru(1)–Ru(2)	2.7557(2)
Ru(1)–H(1)	1.66(2)
Ru(1)–H(2)	1.69(2)
Ru(2)–C(2)	1.811(2)
Ru(2)–Si(1)	2.3781(6)
Ru(2)–Si(4)	2.3790(6)
Ru(2)–Si(3)	2.3791(6)
Ru(2)–Si(2)	2.3822(6)
Ru(2)–Cl	2.5232(5)
Si(1)–C(3)	1.871(3)
Si(1)–C(4)	1.889(3)
Si(1)–H(1)	1.67(2)
Si(2)–C(6)	1.881(3)
Si(2)–C(5)	1.891(2)
Si(2)–H(2)	1.56(2)
Si(3)–C(8)	1.879(3)
Si(3)–C(7)	1.882(3)
Si(3)–N(1)	1.923(2)
Si(4)–C(10)	1.882(3)
Si(4)–C(9)	1.881(3)
Si(4)–N(1)	1.923(2)
Bond angles	
C(1)–Ru(1)–P(1)	95.52(7)
C(1)–Ru(1)–Cl	158.70(7)
P(1)–Ru(1)–Cl	105.757(18)
C(1)–Ru(1)–Si(2)	91.76(8)
P(1)–Ru(1)–Si(2)	127.54(2)
Cl–Ru(1)–Si(2)	76.263(18)
C(1)–Ru(1)–Si(1)	90.30(8)
P(1)–Ru(1)–Si(1)	127.17(2)
Cl–Ru(1)–Si(1)	76.126(19)
Si(2)–Ru(1)–Si(1)	104.60(2)
H(1)–Ru(1)–H(2)	179.3(9)
C(2)–Ru(2)–Si(1)	91.70(7)
C(2)–Ru(2)–Si(4)	91.91(7)
Si(1)–Ru(2)–Si(4)	84.91(2)
C(2)–Ru(2)–Si(3)	92.20(7)
Si(1)–Ru(2)–Si(3)	154.01(2)
Si(4)–Ru(2)–Si(3)	69.29(2)
C(2)–Ru(2)–Si(2)	92.76(7)
Si(1)–Ru(2)–Si(2)	117.02(2)
Si(4)–Ru(2)–Si(2)	157.40(2)
Si(3)–Ru(2)–Si(2)	88.44(2)
Si(1)–Ru(2)–Cl	79.729(19)
Si(4)–Ru(2)–Cl	100.35(2)
Si(3)–Ru(2)–Cl	101.29(2)
Si(2)–Ru(2)–Cl	79.696(19)
Ru(2)–Cl–Ru(1)	66.087(13)
C(3)–Si(1)–C(4)	105.48(14)
C(3)–Si(1)–Ru(2)	121.50(10)
C(4)–Si(1)–Ru(2)	123.69(10)
C(3)–Si(1)–Ru(1)	116.22(10)
C(4)–Si(1)–Ru(1)	118.65(10)
Ru(2)–Si(1)–Ru(1)	67.596(16)
C(3)–Si(1)–H(1)	102.6(8)
C(4)–Si(1)–H(1)	90.7(7)
Ru(2)–Si(1)–H(1)	106.1(6)
Ru(1)–Si(1)–H(1)	39.4(5)
C(6)–Si(2)–C(5)	106.54(12)
C(6)–Si(2)–Ru(2)	121.89(9)
C(5)–Si(2)–Ru(2)	122.89(9)
C(6)–Si(2)–Ru(1)	115.82(10)
C(5)–Si(2)–Ru(1)	117.64(9)
Ru(2)–Si(2)–Ru(1)	67.628(16)
C(6)–Si(2)–H(2)	101.5(8)
C(5)–Si(2)–H(2)	90.1(7)
Ru(2)–Si(2)–H(2)	106.6(6)
Ru(1)–Si(2)–H(2)	39.8(6)

Si(1)–H(1), 1.67(2) and Si(2)–H(2), 1.56(2) Å and can be compared with the mean of the measured non-bridging Si–H distances at 1.393 Å (SD sample, 0.120 Å) [10]. One interpretation of these distances is that in addition to the limiting representation of the bonding as involving a bridging dimethylsilylene and a terminal hydride ligand (structure **G** in Fig. 7) there is also a contribution from a representation in which the Si–H bond of a dimethylsilyl ligand bound to Ru(2), interacts with Ru(1) in an η^2-fashion [11] (structure **H** in Fig. 7). An alternative way of depicting this three-centre bonding interaction is shown as **I** in Fig. 7 which is also the way in which the ORTEP diagram in Fig. 6 is drawn. The unusually small H–P coupling constant in complex **5** (see above) is also consistent with there being some contribution from structure **I**. A related bonding situation, but involving a dirhodium complex with bridging silylene and hydride ligands, has been observed and discussed previously [12].

3. Conclusions

It has been demonstrated that assembly of the very stable dimethylamino-bridged bis(silylene) ligand system, on both ruthenium(II) and osmium(II), is possible through reactions involving the simple silane $HSiMe_2NMe_2$. Previous routes to complexes of this ligand system have involved the use of disilane reagents. Each of the new complexes **1**–**6** has this $L_n\overline{M(SiMe_2NMe_2SiMe_2)}$ formulation. The unusual stability of this ligand system is illustrated by the coexistence of the ligand together with an adjacent hydride ligand in complexes **2** and **4**. The structural parameters of the $\overline{M(SiMe_2NMe_2SiMe_2)}$ ring system are almost constant throughout all the new compounds and suggest a degree of multiple bonding in the M–Si bonds. The unique dinuclear ruthenium complex, $[\overline{Ru(SiMe_2NMe_2SiMe_2)}(CO)(\mu\text{-}\{SiMe_2\})_2(\mu\text{-}Cl)RuH_2(CO)(PPh_3)]$ (**5**), is shown to have a triply bridged structure. Each of the two hydride ligands makes a close approach to one of the silicon atoms of the unsymmetrically bridging dimethylsilylene ligands.

Accordingly, one of the valence bond contributions to the overall bonding involves three-centre interactions between Ru and Si–H bonds.

4. Experimental

4.1. General procedures and instruments

Standard laboratory procedures were followed as have been described previously [9]. The compounds $RuCl(SiMe_2Cl)(CO)(PPh_3)_2$ [9] and $HSiMe_2NMe_2$ [13] were prepared by literature methods.

Infrared spectra (4000–400 cm^{-1}) were recorded as Nujol mulls between KBr plates in a Perkin–Elmer Paragon 1000 spectrometer. NMR spectra were obtained on either a Bruker DRX 400 or Bruker AC 200 at 25 °C. For the Bruker DRX 400, ^{1}H-, ^{13}C-, and ^{29}Si-NMR spectra were obtained operating at 400.1 (^{1}H), 100.6 (^{13}C), and 79.5 (^{29}Si) MHz, respectively. For the Bruker AC 200, ^{1}H- and ^{13}C-NMR spectra were obtained operating at 200.0 (^{1}H) and 50.3 (^{13}C) MHz, respectively. Resonances are quoted in ppm and ^{1}H-NMR spectra referenced to either Me_4Si (0.00 ppm) or the proteo-impurity in the solvent (7.25 ppm for $CHCl_3$). ^{13}C-NMR spectra were referenced to $CDCl_3$ (77.00 ppm) and ^{29}Si-NMR spectra to Me_4Si (0.0 ppm). Elemental analyses were obtained from the Microanalytical Laboratory, University of Otago.

4.2. Preparation of $Os(SiMe_2Cl)Cl(CO)(PPh_3)_2$

$OsHCl(CO)(PPh_3)_2$ (0.200 g, 0.19 mmol) was placed in a Schlenk tube and toluene (10 ml) and $HSiMe_2Cl$ (0.400 g, 4.0 mmol) added. The tube was sealed, cooled in liquid nitrogen and then evacuated. After warming to ambient temperature, the sealed tube was shielded with a safety shield (*caution:* pressure increases as reaction proceeds) and heated in an oil bath at 56 °C for 30 min. During this time the white solid slowly dissolved to give a yellow–orange solution. After cooling, the solvent volume was reduced under vacuum and hexane added slowly to induce crystallisation of a yellow–orange solid. This was collected and recrystallised from dry toluene–hexane to give pure $Os(SiMe_2Cl)Cl(CO)(PPh_3)_2$ (0.160 g, 92%). M.p. 180–183 °C. Anal. Calc. for $C_{39}H_{36}Cl_2OOsP_2Si{\cdot}0.33C_7H_8$: C, 55.00; H, 4.32. Found: C, 54.98; H, 4.34%.

IR (cm^{-1}): 1932, 1918, 1905 (1917 in CH_2Cl_2) ν(CO); 835, 810. ^{1}H-NMR ($CDCl_3$, δ ppm): 0.49 (s, 6H, $Si(CH_3)_2$), 7.25–7.64 (m, 30H, PPh_3). ^{13}C-NMR ($CDCl_3$, δ ppm): 13.2 (s, $Si(CH_3)_2$), 128.2 (t′ [9], $^{2,4}J_{CP} = 9.8$ Hz, *o*-C_6H_5), 130.4 (s, *p*-C_6H_5), 131.6 (t′, $^{1,3}J_{CP} = 50.4$ Hz, *i*-C_6H_5), 134.7 (t′, $^{3,5}J_{CP} = 10.6$ Hz, *m*-C_6H_5), 182.2 (t, $^2J_{CP} = 8.5$ Hz, *C*O).

4.3. Preparation of $\overline{Os(SiMe_2NMe_2}SiMe_2)Cl(CO)(PPh_3)_2$ (1)

$Os(SiMe_2Cl)Cl(CO)(PPh_3)_2$ (0.200 g, 0.23 mmol) was added to dry, degassed benzene (15 ml) in a Schlenk tube and $HSiMe_2NMe_2$ (0.33 g, ~15 mole equivalents) was condensed under vacuum into the Schlenk tube. After sealing the tube, the reaction mixture was allowed to warm to room temperature (r.t.). The sealed tube was then shielded with a safety shield (*caution:* pressure increases as reaction proceeds) and the bright yellow solution was heated in an oil bath held at a temperature of 75 °C for 21 h. The solvent volume was concentrated to approximately 7 ml and dry hexane (10 ml) was carefully layered over the benzene solution by syringe. While standing overnight, large colourless crystals of pure **1** formed (0.086 g, 40%). Although the single crystal selected for X-ray crystal structure analysis proved to have one molecule of benzene per molecule of complex, the results obtained for the sample subjected to elemental analysis required that it was solvated by two molecules of benzene per molecule of complex. Anal. Calc. for $C_{43}H_{48}ClNOOsP_2Si_2{\cdot}2C_6H_6$: C, 60.34; H, 5.52; N, 1.28. Found: C, 60.26; H, 5.67; N, 1.30%. IR (cm^{-1}): 1890 ν(CO). ^{1}H-NMR (C_7D_8, δ ppm): 0.03 (s, 6H, $SiCH_3$), 0.32 (s, 6H, $SiCH_3$), 1.79 (s, 3H, NCH_3), 2.32 (s, 3H, NCH_3), 6.95–7.72 (m, 30H, Ar*H*). ^{13}C-NMR (C_7D_8, δ ppm): −2.00 ($SiCH_3$), 3.11 ($SiCH_3$), 42.17 (NCH_3), 42.82 (NCH_3), 127.58 (m, *o*-C_6H_5), 129.40 (*p*-C_6H_5), 135.37 (t′, $^{3,5}J_{CP} = 10.0$ Hz, *m*-C_6H_5), 137.98 (t′, $^{1,3}J_{CP} = 37.2$ Hz, *i*-C_6H_5). ^{29}Si-NMR (CH_2Cl_2/C_6D_6, δ ppm): 37.85 (dd, $^2J_{SiP(cis)} = 17.4$ Hz, $^2J_{SiP(trans)} = 115.4$ Hz).

4.4. Preparation of $\overline{Os(SiMe_2NMe_2}SiMe_2)H(CO)(PPh_3)_2$ (2)

Complex **2** was synthesised and isolated in a manner similar to that of **1**. Reaction of $Os(SiMe_2Cl)Cl(CO)(PPh_3)_2$ (1.20 g, 1.38 mmol)) and $HSiMe_2NMe_2$ (2.01 g, ~15 mole equivalent) at 90 °C for 24 h gave pure **2** (0.56 g, 45%). Anal. Calc. for $C_{43}H_{49}NOOsP_2Si_2{\cdot}2C_6H_6$: C, 62.30; H, 5.80; N, 1.32. Found: C, 62.06; H, 6.02; N, 1.48%. IR (cm^{-1}): 1859 ν(CO), 1964 ν(OsH). ^{1}H-NMR (C_6D_6, δ ppm): −7.69 (t, 1H, $^2J_{HP} = 17.9$ Hz, Os*H*), −0.34 (s, 6H, $SiCH_3$), 0.60 (s, 6H, $SiCH_3$), 1.77 (s, 3H, NCH_3), 2.26 (s, 3H, NCH_3), 6.87–7.66 (m, 30H, Ar*H*), 7.58–7.66. ^{13}C-NMR ($CDCl_3$, δ ppm): 1.87 ($SiCH_3$), 4.30 (br, $SiCH_3$), 39.90 (NCH_3), 40.21 (NCH_3), 127.05 (t′, $^{2,4}J_{CP} = 8.4$ Hz, *o*-C_6H_5), 128.33 (*p*-C_6H_5), 134.15 (t′, $^{3,5}J_{CP} = 11.4$ Hz, *m*-C_6H_5), 140.41 (t′, $^{1,3}J_{CP} = 40.8$ Hz, *i*-C_6H_5). ^{29}Si-NMR (CH_2Cl_2–C_6D_6, δ ppm): 39.60 (dd, $^2J_{SiP(cis)} = 17.1$ Hz, $^2J_{SiP(trans)} = 89.1$ Hz).

4.5. Preparation of $Ru(SiMe_2NMe_2SiMe_2)Cl(CO)(PPh_3)_2$ (3)

Complex **3** was synthesised and isolated in a manner similar to that of **1**. Reaction of $Ru(SiMe_2Cl)Cl(CO)(PPh_3)_2$ (0.117 g, 0.15 mmol) and $HSiMe_2NMe_2$ (0.235 g, ~15 mole equivalent) at 70 °C for 18 h, gave pure **3** (0.043 g, 34%). Anal. Calc. for $C_{43}H_{48}ClNOP_2RuSi_2 \cdot 1.5C_6H_6$: C, 64.61; H, 5.94; N, 1.45. Found: C, 64.62; H, 6.00; N, 1.09%. IR (cm^{-1}): 1895 ν(CO). ^{1}H-NMR (C_7D_8, δ ppm): 0.05 (br, 6H, SiCH_3), 0.31 (br, 6H, SiCH_3), 1.75 (br, 3H, NCH_3), 2.44 (br, 3H, NCH_3), 6.97–7.72 (m, 30H, ArH). ^{13}C-NMR (C_7D_8, δ ppm): −0.67 (SiCH_3), 4.12 (SiCH_3), 41.90 (NCH_3), 43.37 (NCH_3), 127.80 (br, o-C_6H_5), 128.97 (p-C_6H_5), 135.32 (br, m-C_6H_5), 138.16 (d′ [9], $^{1,3}J_{CP} = 23.1$ Hz, i-C_6H_5), 205.28 (CO). ^{29}Si-NMR (C_7H_8–C_7D_8, δ ppm): 59.83 (dd, $^2J_{SiP(cis)} = 18.1$ Hz, $^2J_{SiP(trans)} = 129.1$ Hz).

4.6. Preparation of $Ru(SiMe_2NMe_2SiMe_2)H(CO)(PPh_3)_2$ (4)

Complex **4** was synthesised and isolated in a manner similar to that of **1**. Reaction of $Ru(SiMe_2Cl)Cl(CO)(PPh_3)_2$ (0.550 g, 0.70 mmol) and $HSiMe_2NMe_2$ (1.02 g, ~15 mole equivalent) at 80 °C for 24 h gave pure **4** (0.229 g, 40% yield). Anal. Calc. for $C_{43}H_{49}NOP_2RuSi_2 \cdot 1.5C_6H_6$: C, 67.00; H, 6.27; N, 1.50. Found: C, 66.86; H, 6.79; N, 1.66%. IR (cm^{-1}): 1918, ν(CO); 1828, ν(RuH). ^{1}H-NMR (C_7D_8, δ ppm): −6.78 (t, 1H, $^2J_{HP} = 16.2$ Hz, RuH), −0.46 (s, 6H, SiCH_3), 0.45 (s, 6H, SiCH_3), 1.81 (s, 3H, NCH_3), 2.33 (s, 3H, NCH_3), 6.92–7.56 (m, 30H, ArH). ^{13}C-NMR ($CDCl_3$, δ ppm): 2.68 (SiCH_3), 5.40 (SiCH_3), 39.78 (NCH_3), 40.45 (NCH_3), 127.12 (br, o-C_6H_5), 128.34 (p-C_6H_5), 134.15 (t′ [9], $^{3,5}J_{CP} = 13.0$ Hz, m-C_6H_5), 140.44 (t′, $^{1,3}J_{CP} = 33.2$ Hz, i-C_6H_5). ^{29}Si-NMR (CH_2Cl_2–C_6D_6, δ ppm): 65.90 (dd, $^2J_{SiP(cis)} = 22.7$ Hz, $^2J_{SiP(trans)} = 100.6$ Hz).

4.7. Preparation of $[Ru(SiMe_2NMe_2SiMe_2)(CO)(\mu\text{-}\{SiMe_2\})_2(\mu\text{-}Cl)RuH_2(CO)(PPh_3)]$ (5)

Complex **5** was isolated as a second crop of crystals from the reaction of $Ru(SiMe_2Cl)Cl(CO)(PPh_3)_2$ (0.550 g, 0.70 mmol) and $HSiMe_2NMe_2$ (1.02 g, ~15 mole equivalent) at 80 °C for 24 h. After removal of **4**, further concentration of the filtrate produced pure **5** as orange crystals (0.059 g, 20%). Anal. Calc. for $C_{30}H_{47}ClNO_2PRu_2Si_4 \cdot 0.33C_6H_6$: C, 44.66; H, 5.74; N, 1.63. Found: C, 44.35; H, 5.63; N, 1.66%. IR (cm^{-1}): 1962, 1896 ν(CO). ^{1}H-NMR (C_7D_8, δ ppm): −6.37 (d, 2H, $^2J_{HP} = 7.2$ Hz, RuH), 0.51 (s, 6H, SiCH_3), 0.55 (s, 6H, SiCH_3), 1.01 (s, 6H, μ-SiCH_3), 1.10 (s, 6H, μ-SiCH_3), 1.80 (s, 3H, NCH_3), 2.08 (s, 3H, NCH_3), 6.98–7.69 (m, ArH). ^{13}C-NMR ($CDCl_3$, δ ppm): 3.44, 3.59 (SiCH_3), 4.94, 4.97, 10.05, 10.10 (μ-SiCH_3), 40.72, 41.00 (NCH_3), 128.15 (d, $^2J_{CP} = 10.4$ Hz, o-C_6H_5), 129.78 (d, $^4J_{CP} = 1.7$ Hz, p-C_6H_5), 133.69 (d, $^3J_{CP} = 13.0$ Hz, m-C_6H_5), 136.68 (d, $^1J_{CP} = 43.8$ Hz, i-C_6H_5). ^{29}Si-NMR (CH_2Cl_2–C_7D_8, δ ppm): 71.05 (s, SiCH_3), 148.60 (d, $^2J_{SiP} = 35.8$ Hz, μ-SiCH_3).

4.8. Preparation of $Ru(SiMe_2NMe_2SiMe_2)Cl(CO)(dppe)$ (6)

Benzene (20 ml) was added to a mixture of $Ru(SiMe_2NMe_2SiMe_2)Cl(CO)(PPh_3)_2$ (0.170 g, 0.20 mmol) and 1,2-bis(diphenylphosphino)ethane (0.080 g, 0.20 mmol). The pale yellow solution was stirred for 30 min and the solvents removed under vacuum. The solid was recrystallised from CH_2Cl_2–hexane to give pure **6** as pale yellow crystals (0.072 mg, 50%). Anal. Calc. for $C_{33}H_{42}ClNOP_2RuSi_2$: C, 54.80; H, 5.85; N, 1.94. Found: C, 54.98; H, 5.88; N, 1.97%. IR (cm^{-1}): 1905 ν(CO). ^{1}H-NMR ($CDCl_3$, δ ppm): 0.14, 0.15, 0.55, 0.56 (s, 12H, SiCH_3), 2.10–2.30 (m, 2H, CH_2), 2.35 (s, 3H, NCH_3), 2.50(s, 3H, NCH_3), 2.66–2.96 (m, 2H, CH_2), 7.23–7.60 (m, 20H, PPh_3). ^{13}C-NMR ($CDCl_3$, δ ppm): 0.90 (SiCH_3), 5.03 (SiCH_3), 27.88 (t′, $^{1,2}J_{CP} = 19.8$ Hz, CH_2CH_2), 42.24 (NCH_3), 43.07 (NCH_3), 127.25–128.26 (m, o-PPh_3), 128.56, 129.35 (s, p-PPh_3), 132.61–132.86 (m, m-PPh_3), 137.19 (d, $^1J_{CP} = 31.5$ Hz, i-PPh_3), 205.39 (t, $^2J_{CP} = 7.1$ Hz, CO).

4.9. X-ray crystal structure determinations for complexes 1, 2, 4–6

X-ray data collection was in a Siemens SMART diffractometer with a CCD area detector, using graphite monochromated Mo–K_α radiation (λ = 0.71073 Å). Data were integrated and Lorentz and polarisation corrections applied using SAINT [14] software. Semi-empirical absorption corrections were applied based on equivalent reflections using SADABS [15]. The structures were solved by Patterson and Fourier methods and refined by full-matrix least squares on F^2 using programs SHELXS [16] and SHELXL [17]. All non-hydrogen atoms were refined anisotropically. Hydrogen atoms other than those bound to the metal were located geometrically and refined with a riding model. The hydrides on the metal were located from electron density maps and their coordinates allowed to refine with thermal parameters 20% greater than the metal atom. In the structure of **1** there was one non-disordered molecule of benzene per molecule of complex and in the structures of **2** and **4** there were two non-disordered molecules of benzene per molecule of complex. Crystal data and refinement details are given in Table 1.

5. Supplementary material

Crystallographic data for the structural analysis have been deposited with the Cambridge Crystallographic Data Centre, CCDC nos. 168872–168876 for **1**, **2**, **4**–**6**, respectively. Copies of this information may be obtained free of charge from The Director, CCDC, 12 Union Road, Cambridge CB2 1EZ, UK (Fax: +44-1223-336033; e-mail: deposit@ccdc.cam.ac.uk or www: http://www.ccdc.cam.ac.uk).

Acknowledgements

We thank the Croucher Foundation, Hong Kong, for supporting this work and for granting a Postdoctoral Fellowship to W.-H.K. We also thank the University of Auckland Research Committee for partial support of this work through grants-in-aid.

References

[1] (a) T.D. Tilley, in: S. Patai, Z. Rappoport (Eds.), The Chemistry of Organic Silicon Compounds, Wiley, New York, 1989, p. 1415 (chap. 24);
(b) T.D. Tilley, in: S. Patai, Z. Rappoport (Eds.), The Silicon–Heteroatom Bond, Wiley, New York, 1991, p. 245 (chaps. 9 and 10; see also p. 309).
[2] W. Buechner, J. Organomet. Chem. Libr. 9 (1980) 409.
[3] (a) M.D. Curtis, P.S. Epstein, Adv. Organomet. Chem. 19 (1981) 213;
(b) M. Kumada, J. Organomet. Chem. 100 (1975) 127.
[4] (a) T.D. Tilley, Acc. Chem. Res. 26 (1993) 22;
(b) H.K. Sharma, K.H. Pannell, Chem. Rev. 95 (1995) 1351.
[5] D.A. Straus, T.D. Tilley, A.L. Rheingold, S.J. Geib, J. Am. Chem. Soc. 109 (1987) 5872.
[6] (a) D.A. Straus, S.D. Grumbine, T.D. Tilley, J. Am. Chem. Soc. 112 (1990) 7801;
(b) S.D. Grumbine, G.P. Mitchell, D.A. Straus, T.D. Tilley, A.L. Rheingold, Organometallics 17 (1998) 5607;
(c) M. Haaf, T.A. Schmedake, R. West, Acc. Chem. Res. 33 (2000) 704;
(d) B. Gehrhus, M.F. Lappert, J. Organomet. Chem. 617–618 (2001) 209.
[7] (a) K. Ueno, H. Tobita, M. Shimoi, H. Ogino, J. Am. Chem. Soc. 110 (1988) 4092;
(b) H. Tobita, K. Ueno, M. Shimoi, H. Ogino, J. Am. Chem. Soc. 112 (1990) 3415;
(c) K. Ueno, H. Tobita, H. Ogino, J. Organomet. Chem. 430 (1992) 93;
(d) J.R. Koe, H. Tobita, H. Ogino, Organometallics 11 (1992) 2479;
(e) K. Ueno, H. Tobita, S. Seki, H. Ogino, Chem. Lett. (1993) 1723;
(f) T. Takeuchi, H. Tobita, H. Ogino, Organometallics 10 (1991) 835;
(g) K. Ueno, A. Masuko, H. Ogino, Organometallics 16 (1997) 5023;
(h) K. Ueno, A. Masuko, H. Ogino, Organometallics 18 (1999) 2694.
[8] G.R. Clark, K.R. Flower, C.E.F. Rickard, W.R. Roper, D.M. Salter, L.J. Wright, J. Organomet. Chem. 462 (1993) 331.
[9] S.M. Maddock, C.E.F. Rickard, W.R. Roper, L.J. Wright, Organometallics 15 (1996) 1793.
[10] Cambridge Crystallographic Data Base, Cambridge Crystallographic Data Centre, www: http://www.ccdc.cam.ac.uk.
[11] U. Schubert, Adv. Organomet. Chem. 30 (1990) 151.
[12] M.D. Fryzuk, L. Rosenberg, S.J. Rettig, Organometallics 15 (1996) 2871.
[13] (a) C. Eaborn, B.N. Ghose, D.R.M. Walton, J. Organomet. Chem. 18 (1969) 371;
(b) S.S. Washburne, W.R. Peterson, J. Organomet. Chem. 21 (1970) 59.
[14] SAINT, Area Detector Integration Software, Siemens Analytical Instruments Inc., Madison, WI, USA, 1995.
[15] G.M. Sheldrick, SADABS, Program for Semi-Empirical Absorption Correction, University of Göttingen, Göttingen, Germany, 1997.
[16] G.M. Sheldrick, SHELXS, Program for Crystal Structure Determination, University of Göttingen, Göttingen, Germany, 1977.
[17] G.M. Sheldrick, SADABS, Program for Crystal Structure Refinement, University of Göttingen, Göttingen, Germany, 1997.